# Robust Stereo Matching Using Probabilistic Laplacian Surface Propagation

Seungryong Kim[1], Bumsub Ham[2⋆], Seungchul Ryu[1], Seon Joo Kim[1], and Kwanghoon Sohn[1]

[1]Yonsei University, Republic of Korea, [2]Inria, France
{srkim89,ryus1,seonjookim,khsohn}@yonsei.ac.kr, {bumsub.ham}@inria.fr

**Abstract.** This paper describes a probabilistic Laplacian surface propagation (PLSP) framework for a robust stereo matching under severe radiometric variations. We discover that a progressive scheme overcomes an inherent limitation for this task, while most conventional efforts have been focusing on designing a robust cost function. We propose the ground control surfaces (GCSs) designed as progressive unit, which alleviates the problems of conventional progressive methods and superpixel based methods, simultaneously. Moreover, we introduce a novel confidence measure for stereo pairs taken under radiometric variations based on the probability of correspondences. Specifically, the PLSP estimates the GCSs from initial sparse disparity maps using a weighted least-square. The GCSs are then propagated on a superpixel graph with a surface confidence weighting. Experimental results show that the PLSP outperforms state-of-the-art robust cost function based methods and other propagation methods for the stereo matching under radiometric variations.

## 1 Introduction

Stereo matching aims to extract 3D scene information by finding the correspondence between stereo pairs taken at different viewpoints of the same scene [1]. Nowadays, state-of-the-art methods provide satisfactory results under the color consistency condition, i.e., corresponding pixels have a similar color distribution. However, the color consistency assumption is often violated since the color of an image is the result of complex combinations of imaging pipelines. Specifically, various factors including illumination source variations, non-Lambertian surfaces, vignetting, device characteristics, and an image noise have an influence on the performance of the stereo matching [2]. Conventionally, to alleviate these problems, a number of methods have been proposed to develop a robust cost function that is insensitive to radiometric distortions [2–7]. However, for stereo images taken under challenging environments, e.g., severe radiometric variations, some pixels or regions cause erroneous local minima. In this case, a robust cost function approach cannot guarantee to estimate reliable correspondences. In addition, costly global optimizations on the Markov random field (MRF), including

⋆ WILLOW project-team, Département d'Informatique de l'Ecole Normale Supérieure, ENS/Inria/CNRS UMR 8548.

a graph-cut (GC) and a belief propagation (BP) [8], cannot also infer a fully reliable solution and even propagate errors under these circumstances.

We discover that a progressive framework can overcome such an inherent limitation for the stereo matching under severe radiometric variations. It is inspired by interactive image editing methods in computer graphics such as colorization [9] and segmentation [10], which propagate an initial seed to infer fully dense results. A number of methods employed the progressive scheme to formulate the stereo matching as a constrained optimization problem [11–13]. These methods find ground control points (GCPs) on reliable regions and propagate them to infer dense disparity maps, which shows satisfactory performance with low complexity. However, an inherent problem of progressive methods is the sensitivity to outliers in initial GCPs since they assume that the initial GCPs are fully reliable [11]. In addition, they induce an edge-blurring on discontinuity regions since a disparity itself is propagated into first-order neighboring pixels. Since the GCPs estimated from stereo images taken under severe radiometric variations cannot be liberated from a false correspondence, conventional progressive methods are not suitable for these tasks.

To alleviate these problems, this paper proposes a probabilistic Laplacian surface propagation (PLSP) framework, which infers an edge-preserved and accurate disparity map even for unreliable GCPs. The PLSP overcomes the limitations of conventional progressive methods by leveraging a superpixel scheme and a confidence weighting. In stereo matching, a superpixel scheme has been popularly incorporated based on the fact that the disparity map is often spatially smooth while its discontinuities are aligned with image edges [14–20]. It reduces an influence of outliers or disparity fluctuations within the superpixel and consolidates boundaries, which enables sharp and accurate disparity maps. However, since slanted-surfaces are defined as three continuous parameters, conventional superpixel based approaches require an inference in continuous MRFs or assign a predefined disparity plane only, which is not robust while demanding a high complexity. The PLSP, combining a progressive scheme and a superpixel scheme, can infer fully continuous slanted-surfaces efficiently. In other words, the PLSP overcomes the limitations of conventional progressive methods and conventional superpixel based methods, simultaneously. Moreover, a novel confidence measure is employed for stereo pairs under radiometric variations, based on the probability of correspondences from initial GCPs. Specifically, the PLSP estimates reliable slanted-surfaces, called the ground control surfaces (GCSs), on superpixels from initial GCPs using a weighted least-square, and propagates these surfaces on a superpixel graph. For the stereo matching under severely different radiometric distortions, the PLSP outperforms other state-of-the-art robust stereo matching methods and propagation methods.

The remainder of this paper is organized as follows. Sec. 2 introduces related works for the proposed method. Sec. 3 describes the PLSP framework for a robust stereo matching. Experimental results are given in Sec. 4. Finally, conclusion and suggestions for future works are given in Sec. 5.

## 2 Related Work

Our approach aims to estimate an accurate disparity map for stereo pairs taken under radiometric variations, and it incorporates a progressive scheme on a superpixel graph. This section describes related works for a robust stereo matching, a progressive stereo matching, and a superpixel based stereo matching.

**Robust Stereo Matching** For a stereo matching under radiometric variations, a number of methods have been proposed to develop a robust cost function [2–7]. A Census transform [3] based on a local order of intensities is tolerant to local illumination variations. It, however, produces unsatisfactory performance on homogeneous or noisy regions where the local order of intensities is indistinct. Although normalized correlation based cost functions such as an adaptive normalized cross-correlation (ANCC) [4] and a Mahalanobis distance cross-correlation (MDCC) [5] show satisfactory results for linear variations, they provide limited performances under severe radiometric distortions. A mutual information (MI) based on the joint probability has been widely used due to its robustness [6, 7]. Hirschmüller and Scharstein evaluated in detail the robustness of cost functions in a stereo matching with respect to various radiometric variations. [2]. Note that any cost function cannot estimate a fully reliable disparity map for stereo pairs taken under severe radiometric variations since there exist the pixels or regions that cause erroneous local minima.

**Progressive Stereo Matching** To address the inherent ambiguities of the stereo matching in homogeneous and occluded areas, progressive approaches have been proposed [11–13]. These methods find reliable disparities on salient pixels, referred as GCPs, and propagate them to neighboring pixels. Sun *et al.* employed a scanline construction with local color and connectivity constraints to propagate reliable disparities [13]. Hawe *et al.* proposed the compressive sensing based propagation scheme [12]. A Laplacian propagation inspired by [9] has been a seminal work due to its robustness [11]. It tried to minimize the difference between a disparity of a center pixel and weighted average of disparities within neighboring pixels [11]. However, conventional progressive approaches have inherent limitations, e.g., they are sensitive to outliers in initial GCPs and induce an edge-blurring especially on discontinuity regions. It is worth noting that unlike these methods, our approach employs a superpixel scheme and a confidence weighting, which provides the edge-preserved disparity maps with the robustness to erroneous GCPs.

**Superpixel Based Stereo Matching** In stereo matching, a superpixel has been popularly incorporated to provide explicit smoothness priors, enforcing all pixels within the superpixel to lie on the same 3D surface [14–20]. These methods first assign an unique slanted-surface for each superpixel by applying the surface fitting to an initial disparity map, such as RANSAC based methods [19], least-square based methods [17], and voting based methods [18, 20]. Then, extracted surfaces are optimized using the BP [18] or the GC [17]. However, the surface fitting is not an easy task when there exist errors on initial correspondences.

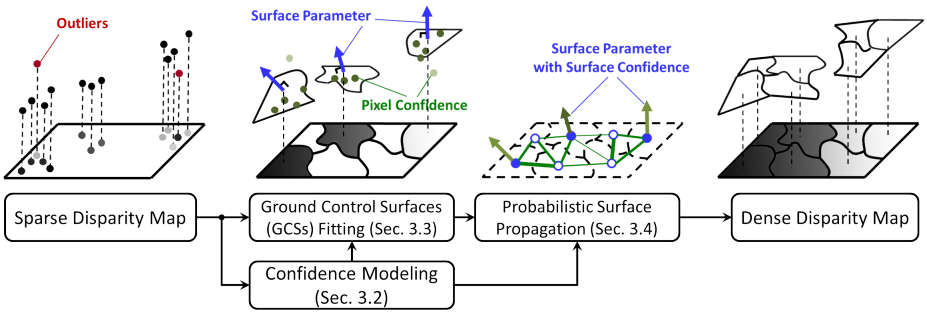


**Fig. 1.** Framework of the PLSP. The PLSP employs a confidence measure based on the probability of correspondences from initial sparse disparity map, and it is used to estimate a slanted-surface as GCSs and a confidence of GCSs itself. The PLSP estimates the GCSs on superpixels from sparse disparity map using a weighted least-square. These slanted-surface parameters are then propagated on a superpixel graph with a surface confidence weighting.

In addition, since slanted-surfaces are defined as three continuous parameters, conventional superpixel based methods require an inference in continuous MRFs to estimate dense slanted-surface maps, which induces a dramatically high complexity [16]. Thus, most methods only assign the label from a predefined disparity plane set on each superpixel, which provides an inherent limitation. Compared to these methods, our approach estimates reliable slanted-surfaces and propagates them on a superpixel graph, which overcomes the limitations of conventional superpixel based methods.

**Contributions of Our Approach** The contributions of this paper are summarized as follows. First, to the best of our knowledge, it is the first attempt to employ a progressive framework for the stereo matching under radiometric variations. Second, instead of propagating the GCPs itself on a pixel graph, our approach propagates the GCSs on a superpixel graph, which overcomes the limitations of conventional progressive methods and conventional superpixel based methods, simultaneously. Finally, a novel confidence measure is proposed for stereo pairs taken under different radiometric conditions based on the probability of correspondences from GCPs, weighted by SIFT features, and it is incorporated into a propagation framework.

## 3 Probabilistic Laplacian Surface Propagation

### 3.1 Problem Statement and Overview

Given stereo pairs $\mathbf{I}_L : \mathcal{I} \rightarrow \mathbb{R}^3$ and $\mathbf{I}_R : \mathcal{I} \rightarrow \mathbb{R}^3$ taken under different radiometric conditions, the PLSP aims to estimate a dense disparity map $\mathbf{D} : \mathcal{I} \rightarrow \mathcal{L}$ that assigns each pixel $\mathbf{m} = [x_\mathbf{m}, y_\mathbf{m}]^\mathbf{T} \in \mathcal{I}$ to a disparity $d_\mathbf{m} \in \mathcal{L}$, where $\mathcal{I} \subset \mathbb{N}^2$ is a dense discrete image domain and $\mathcal{L}$ is a discrete disparity candidate. To this end,

the PLSP leverages a propagation of initial GCPs $\mathbf{G} : \mathcal{I}' \rightarrow \mathcal{L}$, where $\mathcal{I}' \subset \mathcal{I}$ is a sparse discrete image domain. We should note that any given cost function cannot find perfect GCPs for stereo images under severe radiometric variations, thus initial GCPs have non-uniform distributions and erroneous outliers. Fig. 1 shows the overall framework of the PLSP. From the initial GCPs, a disparity confidence is estimated by the probability of correspondences from initial GCPs in Sec. 3.2. Based on this confidence, the PLSP estimates the GCSs from initial GCPs in Sec. 3.3 and propagates these GCSs on the superpixel graph with a surface confidence weighting in Sec. 3.4. Finally, the dense disparity map is fitted by dense slanted-surface parameters.

### 3.2 Confidence Modeling via Color Mapping Probability

In this section, a novel confidence measure is introduced for stereo pairs taken under different radiometric conditions. We argue that the confidence of a disparity at a pixel can be measured by the probability of correspondences between the pixel itself in the left image and the corresponding pixel in the right image. It assumes that there exists a one-to-one color mapping between stereo pairs, i.e., each color in the left image could be mapped into one color in the right image. This assumption explains many instances of color variation such as different camera and different camera setting. It can also explain illumination variations such as global lighting changes and even directional illumination changes [21].

To encode the confidence for a disparity, we leverage that initial GCPs, $\mathbf{G}$, provide the matching relationship between pixel $\mathbf{m} = [x_{\mathbf{m}}, y_{\mathbf{m}}]^{\mathbf{T}}$ in the left image and the corresponding pixel $\hat{\mathbf{m}} = [x_{\mathbf{m}} - d_{\mathbf{m}}, y_{\mathbf{m}}]^{\mathbf{T}}$ in the right image. For all disparities in initial GCPs, the probability of correspondences can be built by computing the joint probability density function (PDF). Since the space of possible color is much bigger than the color distribution of an image, $\mathbf{I}_L$ and $\mathbf{I}_R$ are quantized by $J_L \in \mathcal{J}$ and $J_R \in \mathcal{J}$, respectively, where $\mathcal{J}$ is a set of color indexes, in such a way that the color space is divided into fixed size bins. In addition, to encode a structural similarity between corresponding pixels, the joint PDF is weighted by the difference of SIFT features [22] similar to [7]. The SIFT-weighted joint PDF $p(j_L, j_R)$ is then defined by

$$p(j_L, j_R) = \frac{1}{|\mathcal{I}'|} \sum_{\mathbf{m} \in \mathcal{I}'} \psi(\mathbf{m}, \hat{\mathbf{m}}) T[(j_L, j_R) = (J_L(\mathbf{m}), J_R(\hat{\mathbf{m}}))], \tag{1}$$

where $j_L \in J_L$ and $j_R \in J_R$. $T[\cdot]$ is a logistic operator providing 1 when the argument is true. $|\mathcal{I}'|$ is the total number of pixels in initial GCPs. $\psi(\cdot, \cdot)$ is a SIFT-weighting factor defined by

$$\psi(\mathbf{m}, \hat{\mathbf{m}}) = \exp(-\|\varepsilon_L(\mathbf{m}) - \varepsilon_R(\hat{\mathbf{m}})\|^2 / \lambda_\varepsilon), \tag{2}$$

where $\lambda_\varepsilon$ denotes a coefficient for the degree of structural similarity. $\varepsilon_L(\mathbf{m})$ and $\varepsilon_R(\hat{\mathbf{m}})$ are SIFT features for the pixel $\mathbf{m}$ in the left image and pixel $\hat{\mathbf{m}}$ in the right image, respectively.

Based on the SIFT-weighted joint PDF, a confidence $\mathcal{M}(\mathbf{m}, d_{\mathbf{m}})$ for a pixel $\mathbf{m}$ having a disparity $d_{\mathbf{m}}$ is defined by the bi-directional conditional probability of correspondences between $J_L(\mathbf{m})$ and $J_R(\hat{\mathbf{m}})$ as

$$\mathcal{M}(\mathbf{m}, d_{\mathbf{m}}) \triangleq p(J_L(\mathbf{m})|J_R(\hat{\mathbf{m}}))p(J_R(\hat{\mathbf{m}})|J_L(\mathbf{m})), \tag{3}$$

where $p(J_L(\mathbf{m})|J_R(\hat{\mathbf{m}}))$ and $p(J_R(\hat{\mathbf{m}})|J_L(\mathbf{m}))$ are computed using Baye's theorem and the marginalization as follows:

$$\begin{aligned} p(J_L(\mathbf{m})|J_R(\hat{\mathbf{m}})) &= \frac{p(J_L(\mathbf{m}), J_R(\hat{\mathbf{m}}))}{p(J_R(\hat{\mathbf{m}}))} \\ &= \frac{p(J_L(\mathbf{m}), J_R(\hat{\mathbf{m}}))}{\sum\limits_{\mathbf{k}\in\mathcal{J}} p(\mathbf{k}, J_R(\hat{\mathbf{m}}))}. \end{aligned} \tag{4}$$

After estimating $p(J_R(\hat{\mathbf{m}})|J_L(\mathbf{m}))$ in a similar way, the confidence of disparity in Eq. (3) can be derived as follows:

$$\mathcal{M}(\mathbf{m}, d_{\mathbf{m}}) = \frac{p(J_L(\mathbf{m}), J_R(\hat{\mathbf{m}}))^2}{\sum\limits_{\mathbf{k}\in\mathcal{J}} p(\mathbf{k}, J_R(\hat{\mathbf{m}})) \sum\limits_{\mathbf{k}\in\mathcal{J}} p(J_L(\mathbf{m}), \mathbf{k})}. \tag{5}$$

This novel confidence measure estimates the reliability of disparity, and it is used to estimate a slanted-surface as GCSs and provides a confidence of GCSs itself for a propagation.

### 3.3 Ground Control Surfaces (GCSs)

In order to estimate a slanted-surface parameter of each superpixel from initial GCPs, a number of surface fitting methods can be used [17–20]. Among them, the least-square based approaches provides a slanted-surface fitting with a low computational load [17]. Since the cost function of this method is convex, a closed form solution can be easily found. However, this method is sensitive to outliers. The PLSP employs a weighted least-square for a slanted-surface fitting from initial GCPs on superpixels.

The PLSP uses a graph construction scheme such that every superpixel serves as a graph node and edge is placed between two superpixels if their boundaries have an overlap. Let us denote $i$-th superpixel as $S_i$ and an index set of spatially adjacent superpixels for $S_i$ as $\mathcal{N}_i$. Similar to other superpixel based methods, the PLSP leverages that a slanted-surface for a superpixel $S_i$ represented as $\mathbf{f}_i = [f_i^{\alpha}, f_i^{\beta}, f_i^{\gamma}]^{\mathbf{T}} \in \mathbb{R}^3$ enables an inference of a disparity value of pixel $\mathbf{m} \in S_i$ such that $d_{\mathbf{m}} = \mathbf{a}_{\mathbf{m}}^{\mathbf{T}}\mathbf{f}_i$ where $\mathbf{a}_{\mathbf{m}} = [x_{\mathbf{m}}, y_{\mathbf{m}}, 1]^{\mathbf{T}}$ [14]. The slanted-surface parameter $\mathbf{f}_i^*$ of GCSs is determined as minimizing errors between sparse disparities in initial GCPs and disparities estimated by a slanted-surface within superpixels. The PLSP employs the confidence weighting to reduce an influence of outliers in initial GCPs. In addition, to reduce outliers, a regularization term is employed. Thus, our energy function $\Phi_i(\mathbf{f})$ is defined as follows:

$$\Phi_i(\mathbf{f}) = \sum_{\mathbf{m}\in S_i\cap\mathcal{I}'} \mathcal{M}(\mathbf{m}, d_{\mathbf{m}})(d_{\mathbf{m}} - \mathbf{a}_{\mathbf{m}}^{\mathbf{T}}\mathbf{f})^2 + \lambda_f \mathbf{f}^{\mathbf{T}}\mathbf{f}, \tag{6}$$

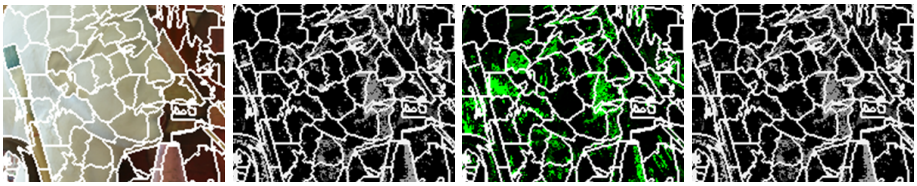

(a) (b) (c) (d)

**Fig. 2.** The GCSs fitting from initial GCPs for *Art* image pairs. (a) Superpixel decompositions for a reference image. (b) Initial GCPs $\mathbf{G}$ with the superpixel grid. (c) Confidence weights $\mathcal{M}(\mathbf{m}, d_{\mathbf{m}})$ for initial GCPs. The degree of the confidence is indicated as the brightness of green color. (d) The GCSs fitting as $\mathbf{f}_i^*$. The GCSs fitting on superpixels reduces the influence of erroneous GCPs. These GCSs can be a soft constraint for dense slanted-surface maps.

where $\lambda_f$ is a regularization parameter. It can be represented as the matrix-vector form as

$$\Phi_i(\mathbf{f}) = (\mathbf{D} - \mathbf{A}\mathbf{f})^{\mathbf{T}}\mathbf{M}(\mathbf{D} - \mathbf{A}\mathbf{f}) + \mathbf{f}^{\mathbf{T}}\mathbf{\Lambda}\mathbf{f}, \tag{7}$$

where $\mathbf{M} = diag\{\mathcal{M}(\mathbf{m}, d_{\mathbf{m}})\}_{\mathbf{m}\in S_i \cap \mathcal{I}'}$, $\mathbf{\Lambda} = diag\{\lambda_f\}$, $\mathbf{D} = \{d_{\mathbf{m}}\}_{\mathbf{m}\in S_i \cap \mathcal{I}'}$, and $A = \{\mathbf{a}_{\mathbf{m}}^{\mathbf{T}}\}_{\mathbf{m}\in S_i \cap \mathcal{I}'}$. The slanted-surface parameter, minimizing this energy function, can be estimated by $\nabla\Phi_i(\mathbf{f}) = 0$ as in Eq. (8).

$$\mathbf{f}_i^* = (\mathbf{A}^{\mathbf{T}}\mathbf{M}\mathbf{A} + \mathbf{\Lambda})^{-1}\mathbf{A}^{\mathbf{T}}\mathbf{M}\mathbf{D}. \tag{8}$$

In order to eliminate erroneous surface parameters, appearance neighbors are employed similar to [15]. Given a superpixel $S_i$, we search the neighboring superpixels having similar appearances by estimating a superpixel feature affinity, which will be described in the following section, within a predefined window. Let $\mathcal{N}_i^s$ is an index set of these superpixels. Our approach eliminates a non-reliable superpixel satisfying that

$$\left\| \mathbf{f}_i^* - \frac{1}{|\mathcal{N}_i^s|} \sum_{j\in\mathcal{N}_i^s} \mathbf{f}_j^* \right\| < \tau_s, \tag{9}$$

where $|\mathcal{N}_i^s|$ is the number of appearance neighbors, and $\tau_s$ is a threshold. Finally, the slanted-surface represented by a parameter $\mathbf{f}_i^*$ is defined as ground control surfaces (GCSs). We use these GCSs as initial sparse surfaces to provide the soft constraint for the propagation.

Fig. 2 shows the GCSs fitting from initial GCPs for *Art* image pairs. As shown in GCPs, initial disparities are non-uniformly distributed with outliers. For the GCSs fitting, the reference image is decomposed as non-overlapping superpixels. Based on superpixels, the PLSP estimates a reliable slanted-surface on each superpixel with the confidence weighting, which consolidates disparity boundaries and reduces the influence of outliers in initial GCPs.

### 3.4 Optimization Framework

The PLSP formulates an inference of a set of piecewise continuous slanted-surfaces as a constrained optimization problem where the GCSs are interpreted as soft constraints. It formulates each energy function for slanted-surface parameters $f_i^{\alpha}$, $f_i^{\beta}$, and $f_i^{\gamma}$ and minimizes these functions, independently. Let $\mathbf{F} = \{f_i\}$ be the vector of all slanted-surface parameters for superpixels. The energy function of the PLSP is defined as follows:

$$\mathbf{E}(\mathbf{F}) = \mathbf{E}_{data}(\mathbf{F}) + \mathbf{E}_{smooth}(\mathbf{F}), \tag{10}$$

where a data term $\mathbf{E}_{data}(\mathbf{F})$ and a smoothness term $\mathbf{E}_{smooth}(\mathbf{F})$ are defined as

$$\mathbf{E}_{data}(\mathbf{F}) = \sum_i p_i (f_i - f_i^*)^2, \tag{11}$$

$$\mathbf{E}_{smooth}(\mathbf{F}) = \sum_i \sum_{j \in \mathcal{N}_i} \omega_{ij} (f_i - f_j)^2. \tag{12}$$

$\mathbf{E}_{data}(\mathbf{F})$ encodes the penalty for the dissimilarity of slanted-surface parameters $f_i$ and corresponding parameters $f_i^*$ for GCSs. In addition, it encodes a surface confidence weight $p_i$ to reduce the influence of erroneous GCSs according to the reliability of surface. $\mathbf{E}_{smooth}(\mathbf{F})$ imposes the constraint that two adjacent superpixel $i$ and $j$ have similar slanted-surface parameters according to surperpixel feature affinity $\omega_{ij}$, which will be detailed in the following section.

**Confidence for Ground Control Surfaces** While conventional propagation methods impose an uniform confidence for initial seeds, the PLSP employs a confidence weighting for GCSs according to the reliability of GCSs. The GCSs represented as $\mathbf{f}_i^*$ enable an inference of the disparity value of pixels $\mathbf{m} \in S_i$ such that $\mathbf{a}_\mathbf{m}^\mathbf{T}\mathbf{f}_i^*$. Thus, a confidence for pixels within a superpixel is computed as $\mathcal{M}(\mathbf{m}, \mathbf{a}_\mathbf{m}^\mathbf{T}\mathbf{f}_i^*)$. In order to estimate a surface confidence weight $p_i$ of GCSs, these confidence weights are aggregated within a superpixel $S_i$ as

$$p_i = \frac{1}{|S_i|} \sum_{\mathbf{m} \in S_i} \mathcal{M}(\mathbf{m}, \mathbf{a}_\mathbf{m}^\mathbf{T}\mathbf{f}_i^*), \tag{13}$$

where $|S_i|$ is the number of pixels within a superpixel $S_i$. This surface confidence weight enables the propagation of initial GCSs according to their reliability, thus reducing the influence of erroneous GCSs in a propagation procedure.

**Superpixel Feature Affinity** A superpixel as a propagation unit can encode regional features, providing more robust affinity between adjacent superpixels compared to the intensity feature into first-order neighboring pixels in conventional methods [11]. The PLSP employs a superpixel feature composed of a color appearance, a SIFT feature, and a spatial feature. First, color appearance feature $\upsilon_i^c$ describes statistical color information as the average and standard deviation

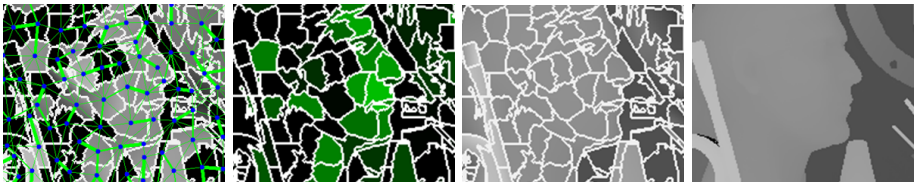

(a) (b) (c) (d)

**Fig. 3.** Propagation of the GCSs in Fig. 2 on a superpixel graph. (a) The superpixel graph (blue dot: node, green line: edge with superpixel affinities $\omega_{ij}$.) (b) Surface confidence weights $p_i$ for GCSs. The degree of the confidence is indicated as the brightness of green color. (c) Results of the PLSP. (d) Ground truth. The PLSP propagates reliable GCSs on the superpixel graph with the surface confidence weighting, which provides an edge-preserved and accurate disparity map.

for pixels within superpixels in RGB, Lab, and YCbCr color space [23]. Second, in order to encode structural information, we adopt the SIFT feature $v_i^s$ [22]. Specifically, dense SIFT features are extracted from pixels, and then, these features are aggregated within superpixels. Finally, spatial feature $v_i^p$ is defined as a spatial centroid coordinate within superpixels.

Based on these superpixel features, a superpixel feature affinity $\omega_{ij}$ between adjacent superpixel $i$ and $j$ is computed as

$$\omega_{ij} \propto \exp(-\left\|v_i^c - v_j^c\right\|^2/\lambda_c - \left\|v_i^s - v_j^s\right\|^2/\lambda_s - \left\|v_i^p - v_j^p\right\|^2/\lambda_p), \tag{14}$$

where $\lambda_c$, $\lambda_s$, and $\lambda_p$ denote coefficients for the similarity degree measuring a coherence of neighboring superpixels. The larger $\omega_{ij}$ is, the more likely that two neighboring superpixels have same slanted-surfaces. The affinity $\omega_{ij}$ is normalized to have a unit sum such that

$$\sum_{j \in \mathcal{N}_i} \left\|\omega_{ij}\right\|^2 = 1. \tag{15}$$

**Solver** One strength of our approach is the low complexity since no costly global optimizations are required such as the GC and the BP [8]. The energy function $\mathbf{E}(\mathbf{F})$ in Eq. (10) can be expressed in matrix-vector form as

$$\mathbf{E}(\mathbf{F}) = (\mathbf{F} - \mathbf{F}^*)^\mathbf{T}\mathbf{P}(\mathbf{F} - \mathbf{F}^*) + \mathbf{F}^\mathbf{T}(\mathbf{L} - \mathbf{W})\mathbf{F}, \tag{16}$$

where $\mathbf{F}^*$ is the vector of surface parameters of GCSs. The matrix $\mathbf{P}$ is a diagonal matrix whose diagonal elements with surface confidence weights such that $\mathbf{P}_{ii} = p_i$. The matrix $\mathbf{L}$ is an identity matrix. The matrix $\mathbf{W}$ is a weight matrix whose elements are pairwise affinities $\omega_{ij}$.

The minimum of this discrete quadratic form can be obtained by setting $\nabla\mathbf{E}(\mathbf{F}) = 0$, which amounts to solving the following linear system as

$$(\mathbf{P} + \mathbf{L} - \mathbf{W})\mathbf{F} = \mathbf{P}\mathbf{F}^*. \tag{17}$$

**Algorithm 1**: Probabilistic Laplacian Surface Propagation

**Input** : stereo pairs $\mathbf{I}_L$, $\mathbf{I}_R$, and GCP $\mathbf{G}$.

**Output** : dense disparity map $\mathbf{D}$.

**1:** Compute a confidence of disparity $\mathcal{M}(\mathbf{m}, d_{\mathbf{m}})$ as in Eq. (5) from GCPs $\mathbf{G}$.

**2:** Decompose the reference image $\mathbf{I}_L$ into superpixels $S_i$.

**3:** Estimate the parameter of GCSs $\mathbf{f}_i^* = [f_i^\alpha, f_i^\beta, f_i^\gamma]^\mathbf{T}$ as in Eq. (8).

**4:** Compute a Laplacian matrix $\mathbf{P} + \mathbf{L} - \mathbf{W}$ with surface confidence weights $p_i$ in Eq. (13) and affinities $\omega_{ij}$ in Eq. (14) .

**5:** Estimate the slanted-surface parameters by $\mathbf{F} = (\mathbf{P} + \mathbf{L} - \mathbf{W})^{-\mathbf{1}}\mathbf{P}\mathbf{F}^*$ in Eq. (17) where $\mathbf{F}^* = [\mathbf{F}_\alpha^*, \mathbf{F}_\beta^*, \mathbf{F}_\gamma^*]$.

**6:** Estimate the dense disparity map $\mathbf{D}$ such that $d_{\mathbf{m}} = \mathbf{a}_{\mathbf{m}}^\mathbf{T}\mathbf{f}_i$ for all superpixels.

This linear system with a laplacian matrix can be easily solved as conventional linear solvers [24]. Compared to propagation on a pixel graph [11], our approach can reduce the computational complexity of the linear solver with the proposition to the number of pixels within superpixels.

Fig. 3 (a) shows the superpixel graph constructed by superpixel feature affinities, and Fig. 3 (b) shows the surface confidence weight. In the PLSP, the GCSs are propagated on the superpixel graph with the confidence weighting to infer dense disparity maps as in Fig. 3 (c). The PLSP is summarized in Algorithm 1.

## 4 Experimental Results

In this section, the stereo matching performance is evaluated for the PLSP and other methods on the Middlebury datasets [2], where each dataset consists of stereo image pairs taken under varying illumination conditions indexed from 1 to 3 and exposure conditions indexed from 0 to 2. In order to evaluate the robustness to radiometric variations, stereo images were selected according to the index of illumination or exposure, e.g., "illumination combination 1/1" was defined as an index of illumination varying from 1 to 1 [2]. The PLSP was compared with the state-of-the-art robust stereo matching methods such as the MI [6], Census transform [3], the NCC [2], and the ANCC [4]. These methods were optimized with the graph-cut (GC) as in [4]. In addition, since the PLSP was designed to propagate initial GCPs to infer dense disparity map, it was also compared with other propagation methods for fixed GCPs, such as a weighted median filtering (WMF) with a hole filling [25], a Guided filtering (GF) based propagation [26, 24], and a Laplacian propagation (LP) [11]. To evaluate the robustness of proposed confidence measure, the LP combined with a confidence weighting (PLP) was evaluated. To evaluate the robustness of the GCSs scheme, the Laplacian surface propagation (LSP)[1] was also evaluated. The parameters of each method were set to the same values from the original works. The evaluation criterion is the bad pixel error rate in the non-occluded areas of disparity maps since it has been popularly used in stereo literatures [4].

[1] In order to evaluate the robustness of only surface propagation, the LSP only expands the propagation unit as a superpixel without the confidence weighting for GCSs.

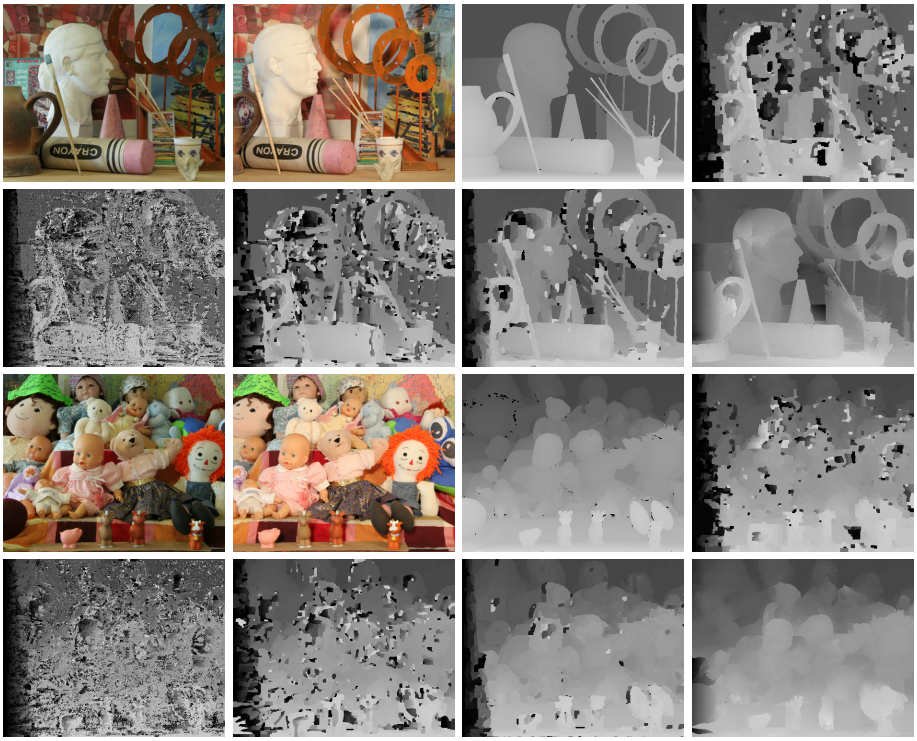

**Fig. 4.** Comparison of disparity estimation for *Art* and *Dolls* image pairs taken under illumination combination 1/3. (from left to right, from top to bottom) Left color image, right color image, and disparity maps for the ground truth, MI+GC [6], Census+GC [3], NCC+GC [2], ANCC+GC [4], and PLSP. Conventional robust cost functions cannot estimate a fully reliable correspondence even with a global optimization. In contrast, the PLSP estimates accurate disparity maps.

In the experiments, similar to other methods detecting the GCPs [11–13], initial GCPs were estimated by a linear combination of cost functions, the NCC [2] and the Census [3], with a winner-takes-all (WTA) optimization and refined by left-right cross-check [13]. For the superpixel graph, the reference image was decomposed by a SLIC superpixel due to its compactness and regular shape [27], and the number of superpixels was set to from 1000 to 1500. The structural similarity coefficient was defined as $\lambda_\varepsilon = 1.3$. The color space was quantized as bin size $20 \times 20 \times 20$ in all experiments. For superpixel feature affinity, the parameters were empirically determined as $\{\lambda_c, \lambda_s, \lambda_p\} = \{0.036, 1.6, 12.8\}$.

### 4.1 Comparison with Robust Stereo Matching Methods

In order to evaluate the robustness for radiometric variations, disparity maps of the PLSP and other robust stereo matching methods were estimated for stereo pairs taken under radiometric variations. Fig. 4 shows disparity maps for *Art*

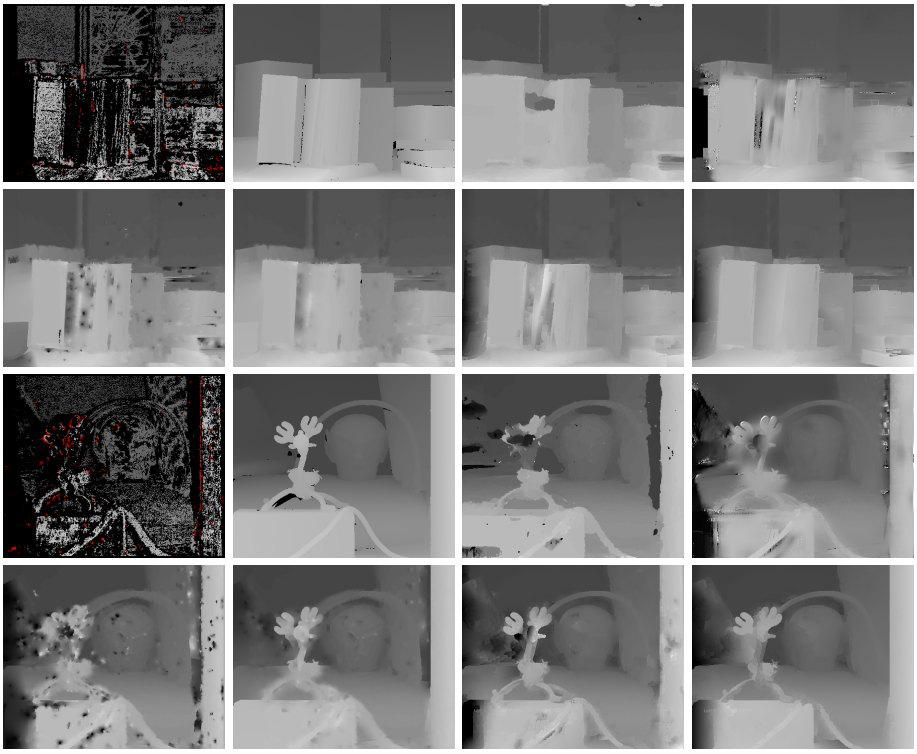

**Fig. 5.** Comparison of disparity propagation for GCPs from *Books* and *Reindeer* image pairs taken under illumination combination 1/3. (from left to right, from top to bottom) The initial GCPs and disparity maps for the ground truth, WMF with the hole filling [25], GF-based propagation [26], LP [11], PLP, LSP, and PLSP. Conventional methods show the limitation for unreliable GCPs. Disparity maps of PLP, LSP, and PLSP show that a superpixel scheme with the confidence weighting provides an edge-preserved and accurate disparity map.

and *Dolls* stereo images under the illumination combination 1/3, which is the most severe radiometric variation.

The performance of the MI-based method is degraded under local variations, since it is assumed that there are global variations. In addition, the Census transform provides poor results on homogeneous regions which have an indistinct order of intensities. The normalized correlation based methods such as the NCC and the ANCC show high performance compared to the Census transform. However, disparity maps of the NCC contain large errors in boundary regions since it does not encode the spatial structure. The ANCC improves the matching performance using weight distributions compared to the NCC. However, conventional approach for these tasks show the limitations. Pixels degraded by severe radiometric distortions are not estimated perfectly by robust cost functions even with a global optimization. In contrast, the PLSP outperforms conventional methods by addressing these problems. Since the PLSP propagates sparse and reliable

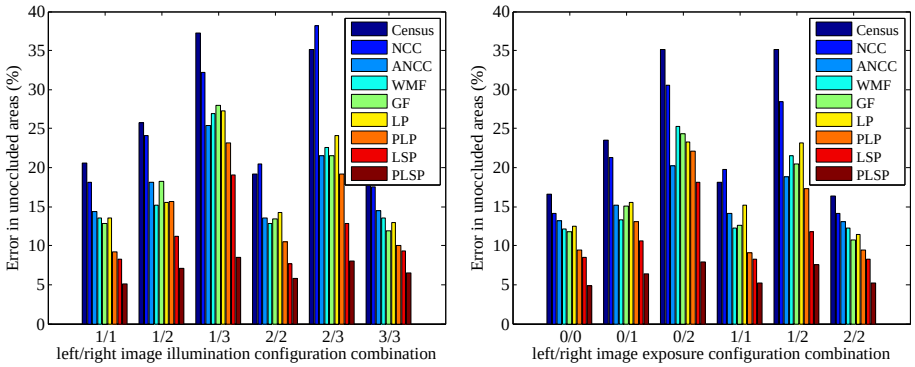


(a) (b)

**Fig. 6.** Average bad pixel error rates in the un-occluded areas for disparity maps from *Art*, *Baby1*, *Books*, *Bowling2*, *Cloth3*, *Cloth4*, *Dolls*, *Moebius*, *Reindeer*, and *Wood1* with varying the combination of illumination and exposure index. (a) Illumination variations. (b) Exposure variations. Progressive approaches including WMF [25], GF [26], LP [11], PLP, LSP, and PLSP relatively outperform conventional robust cost function based approaches such as Census [3], NCC [2], and ANCC [4]. The PLSP shows the best performance with the lowest bad pixel error rates.

GCSs without estimating erroneous pixels, it fills these erroneous regions by propagating reliable regions.

### 4.2 Comparison with Robust Propagation Methods

In this section, the PLSP was compared with different robust propagation methods in terms of stereo matching under radiometric variations. For the fair comparison, the initial GCPs were fixed in all methods. Fig. 5 shows disparity maps of different propagation methods for the GCPs estimated from *Books* and *Reindeer* image pairs under the illumination combination 1/3.

As shown in Fig. 5, initial GCPs have erroneous disparities and non-uniform distributions, which induces large hole regions on discontinuity regions. Although the WMF with the hole filling have shown the satisfactory performance in disparity refinements, it cannot estimate accurate dense disparity for erroneous GCPs, especially on large holes. The GF-based propagation provides more edge-preserved disparity maps compared to other methods. However, it is also sensitive to outliers of initial GCPs. In addition, since the GF uses a reference color image, the textures in the color image are also propagated in final disparity maps. As the most related method, the LP induces edge blurring and propagates erroneous initial GCPs, since it propagates disparity itself on a pixel graph without the consideration of the disparity confidence. In contrast, the LP with proposed confidence weighting, PLP, reduces an influence of the erroneous pixels. However, there still exists edge blurring problems. Compared to the pixel propagation, the Laplacian surface propagation, LSP, preserves disparity discontinuities. However, it cannot refine erroneous superpixels. The PLSP framework

consisting of the surface propagation with the confidence weighting shows the best performance. It dramatically reduces an influence of errors in initial GCPs and provides edge-preserved disparity maps compared with other methods.

Fig. 6 shows average bad pixel error rates of disparity maps from *Art*, *Baby1*, *Books*, *Bowling2*, *Cloth3*, *Cloth4*, *Dolls*, *Moebius*, *Reindeer*, and *Wood1* with varying the combination of illumination and exposure index. Most propagation methods relatively outperform robust cost function based methods since they propagate the GCPs without estimating erroneous pixels. However, since there still remain outliers on initial GCPs from stereo pairs under radiometric variations, conventional propagation methods provide the limited performance. In contrast, the PLSP shows the best performance with the lowest bad pixel error rates compared to other methods. In addition, the PLSP shows competitive performances for stereo pairs under normal conditions without radiometric variations. More experimental results are available in the supplementary materials.

## 5 Conclusion

The robust stereo matching framework called the PLSP has been proposed for the stereo matching under severe radiometric variations. We discover that a progressive framework overcomes the limitation of conventional approaches for these tasks. Instead of propagating the GCPs itself on the pixel graph, we introduced the GCSs as a propagation unit. To measure the confidence of a disparity for stereo pairs under radiometric variations, a novel confidence measure has been proposed based on the probability of correspondence from initial GCPs. The PLSP provides an edge-preserved disparity map while reducing the influence of outliers in initial GCPs. Experimental results have shown that the PSLP outperforms state-of-the-art robust stereo matching methods and propagation methods for stereo image pairs taken under severely different radiometric conditions.

For future work, the PLSP will be applied to address other correspondence problems under different radiometric conditions, such as optical flow or dense image alignment.

**Acknowledgement**. This research was supported by the MSIP(Ministry of Science, ICT and Future Planning), Korea, under the ITRC(Information Technology Research Center) support program (NIPA-2014-H0301-14-1012) supervised by the NIPA(National IT Industry Promotion Agency).

## References

1. Scharstein, D., Szeliski, R.: A taxonomy and evaluation of dense two-frame stereo correspondence algorithms. IJCV **47** (2002) 7–42
2. Hirschmüller, H., Scharstein, D.: Evaluation of stereo matching costs on images with radiometric differences. TPAMI **31** (2009) 1582–1599
3. Zabih, R., Woodfill, J.: Non-parametric local transforms for computing visual correspondence. In: ECCV (1994)

4. Heo, Y., Lee, K., Lee, S.: Robust stereo matching using adaptive normalized cross-correlation. TPAMI **33** (2011) 807–822
5. Kim, S., Ham, B., Kim, B., Sohn, K.: Mahalanobis distance cross-correlation for illumination invariant stereo matching. TCSVT (2014) to be published.
6. Kim, J., Kolmogorov, V., Zabih, R.: Visual correspondence using energy minimization and mutual information. In: ICCV (2003)
7. Heo, Y., Lee, K., Lee, S.: Mutual information-based stereo matching combined with sift descriptor in log-chromaticity color space. In: CVPR (2009)
8. Szeliski, R., Zabih, R., Scharstein, D., Veksler, O., Kolmogorov, V., Agarwala, A., Tappen, M., Rother, C.: A comparative study of energy minimization methods for markov random fields. In: ECCV (2008)
9. Levin, A., Lischinski, D., Weiss, Y.: Colorization using optimization. In: SIGGRAPH (2006)
10. Krishnan, D., Fattal, R., Szeliski, R.: Efficient preconditioning of laplacian matrices for computer graphics. In: SIGGRAPH (2013)
11. Wang, L., Yang, R.: Global stereo matching leveraged by sparse ground control points. In: CVPR (2011)
12. Hawe, S., Kleinsteuber, M., Diepold, K.: Dense disparity maps from sparse disparity measurements. In: ICCV (2011)
13. Sun, X., Mei, X., Zhou, M., Wang, H.: Stereo matching with reliable disparity propagation. In: 3DIMPVT (2011)
14. Yamaguchi, K., Hazan, T., McAllester, D., Urtasun, R.: Continuous markov random fields for robust stereo estimation. In: ECCV (2012)
15. Lu, J., Yang, H., Min, D., Do, M.: Patchmatch filter: Efficient edge-aware filtering meets randomized search for fast correspondence field estimation. In: CVPR (2013)
16. Bleyer, M., Rother, C., Kohli, P.: Surface stereo with soft segmentation. In: CVPR (2010)
17. Hong, L., Chen, G.: Segment-based stereo matching using graph cuts. In: CVPR (2004)
18. Klaus, A., Sormann, M., Karner, K.: Segment-based stereo matching using belief propagation and a self-adapting dissimilarity measure. In: ICPR (2006)
19. Sinha, S., Steedly, D., Szeliski, R.: Piecewise planar stereo for image-based rendering. In: ICCV (2009)
20. Wang, Z., Zheng, Z.: A region based stereo matching algorithm using cooperative optimization. In: CVPR (2008)
21. Hwang, Y., Lee, J., Kweon, I., Kim, S.: Color transfer using probabilistic moving least squares. In: CVPR (2014)
22. Lowe, D.: Distinctive image features from scale-invariant keypoints. IJCV **60** (2004) 91–110
23. Chia, A., Zhuo, S., Gupta, R., Tai, Y., Cho, S., Tan, P., Lin, S.: Semantic colorization with internet images. In: SIGGRAPH (2011)
24. Lang, M., Wang, O., Aydic, T., Smolic, A., Gross, M.: Practical temporal consistency for image-based graphics applications. In: SIGGRAPH (2012)
25. Ma, Z., He, K., Wei, Y., Sun, J., Wu, E.: Constant time weighted median filtering for stereo matching and beyond. In: ICCV (2013)
26. He, K., Sun, J., Tang, X.: Guided image filtering. In: ECCV (2010)
27. Achanta, R., Shaji, A., Smith, K., Lucchi, A., Fua, P., Susstrunk, S.: SLIC superpixels compared to state-of-the-art superpixel methods. TPAMI **34** (2012) 2274–2282